

Observation of the Galactic Cosmic Ray Moon shadowing effect with the ARGO-YBJ experiment

Roberto Iuppa^{* †}, Daniele Martello^{‡§}, Bo Wang[¶] and Giovanni Zizzi^{‡§}
on behalf of the ARGO-YBJ Collaboration

^{*} INFN Sezione Roma Tor Vergata, via della Ricerca Scientifica 1, Rome - Italy

[†] Dipartimento di Fisica, Università Roma Tor Vergata, via della Ricerca Scientifica 1, Rome - Italy

[‡] INFN Sezione di Lecce, via per Arnesano, 73100 Lecce - Italy

[§] Dipartimento di Fisica dell'Università del Salento, via per Arnesano, 73100 Lecce - Italy

[¶] Key Laboratory of Particle Astrophysics, IHEP - Chinese Academy of Science, P.O. Box 918, 100049 Beijing, P.R. China

Abstract. Cosmic rays are hampered by the Moon and a deficit in its direction is expected (the so-called *Moon shadow*). The Moon shadow is an important method to determine the performance of an air shower array. In fact, the westward displacement of the shadow center, due to the propagation of cosmic rays in the geomagnetic field, allows to calibrate the energy scale of the primary particles observed by the detector. In addition, the shape of the shadow allows a measurement of the angular resolution and the position of the deficit at high energy allows the evaluation of the pointing accuracy of the detector.

In this paper we present the observation of the galactic cosmic rays Moon shadowing effect performed by the ARGO-YBJ experiment in the multi-TeV energy region. The measured angular resolution as a function of the shower size is compared with the expectations from a MC simulation.

Keywords: Moon Shadow observation, Cosmic Rays, ARGO-YBJ experiment

I. INTRODUCTION

The angular resolution is a critical feature of an Extensive Air Shower (EAS) array in gamma-ray astronomy. In fact, the rejection of the nearly isotropic background of charged cosmic rays is mainly performed by improving the angular resolution, thus reducing the source region extension. Hence the tuning of a firm calibration technique of the angular resolution is mandatory.

The CYGNUS experiment in 1991 reported the first determination of the angular resolution of an EAS detector by exploiting the analysis of the shadow of the Moon [1]. In fact, as pointed out in 1957 by Clark [2], the cosmic rays are hampered in their propagation to the Earth due to the Moon's presence and a deficit of events in its direction is expected: the so-called *Moon shadow*.

At high energy, the Moon shadow would be observed by an ideal detector as a 0.26° wide circular deficit of events, centered on the Moon position. The deviation from such an ideal case gives us information about the Point Spread Function (PSF) of the detector. The shape of the deficit allows the measurement of the angular

resolution and its position allows the evaluation of the absolute pointing accuracy of the detector. In addition, positively charged particles are eastward deflected, due to the geomagnetic field, with an energy dependence $\Delta\theta \sim 1.6^\circ Z/E_{TeV}$. As a consequence, the observation of the displacement of the Moon provides a direct check of the relation between shower size and primary energy. Therefore, the analysis of the Moon shadow allows the calibration of the performance of an EAS array.

The same shadowing effect can be observed in the direction of the Sun but the interpretation of the shadowing phenomenology is more complex. In fact, the displacement of the shadow from the apparent position of the Sun could be explained by the joint effects of the geomagnetic field and of the solar and Interplanetary Magnetic Fields, whose configuration considerably changes with the phases of the solar activity cycle [3]. Results about the Sun shadow observation with the ARGO-YBJ experiment are discussed in [4].

In this paper we present the observation of the galactic cosmic rays Moon shadowing effect carried out by the ARGO-YBJ experiment. We report on the angular resolution of the detector in the multi-TeV energy region. The pointing error is also investigated.

II. THE ARGO-YBJ EXPERIMENT

The ARGO-YBJ detector, located at the YangBaJing Cosmic Ray Laboratory (Tibet, P.R. China, 4300 m a.s.l.), is the only experiment exploiting the *full coverage* approach at very high altitude. The detector is constituted by a central carpet $\sim 74 \times 78$ m², made of a single layer of Resistive Plate Chambers (RPCs) with $\sim 92\%$ of active area, enclosed by a partially instrumented guard ring that extends the detector surface up to $\sim 100 \times 110$ m². The apparatus has a modular structure, the basic data acquisition element being a cluster (5.72×7.64 m²), namely a group of 12 RPCs (2.80×1.25 m² each). Each chamber is read by 80 strips of 7×62 cm² (the spatial pixel), logically organized in 10 independent pads of 56×62 cm² representing the time pixel of the detector. The RPCs are operated in streamer mode with a standard gas mixture (Argon 15%, Isobutane 10%,

TetraFluoroEthane 75%), the High Voltage settled at 7.2 kV ensures an overall efficiency of about 96% [5]. The central carpet contains 130 clusters (hereafter ARGO-130) and the full detector is composed of 153 clusters for a total active surface of $\sim 6700 \text{ m}^2$.

All events giving a number of fired pads $N_{pad} \geq N_{trig}$ in the central carpet within a time window of 420 ns are recorded. The spatial coordinates and the time of any fired pad are then used to reconstruct the position of the shower core and the arrival direction of the primary.

The ARGO-YBJ experiment started recording data with the whole central carpet in June 2006. Since 2007 November the full detector is in stable data taking at the multiplicity trigger threshold $N_{trig} \geq 20$ and a duty cycle $\sim 90\%$: the trigger rate is about 3.6 kHz.

The reconstruction of shower parameters is split into the following steps. First the shower core position is derived with the Maximum Likelihood method from the lateral density distribution of the secondary particles. In the second step, given the shower core position, the shower axis is reconstructed by means of an iterative weighted planar fit being able to reject the time values belonging to the non-gaussian tails of the arrival time distributions. A conical correction with a slope fixed to $\alpha = 0.03 \text{ rad}$ is applied to the surviving hits in order to improve the angular resolution [6].

III. MONTE CARLO SIMULATION

The air showers development in the atmosphere has been generated with the CORSIKA v. 6.500 code including the QGSJET-II.03 hadronic interaction model for primary energy above 80 GeV and the FLUKA code for lower energies [7]. Cosmic ray spectra of p, He and CNO have been simulated in the energy range from 30 GeV to 1 PeV following [8]. The relative fractions (in % of the total) after triggering by the ARGO-YBJ detector for events with $N_{strip} \geq 30$ are: p $\sim 88\%$, He $\sim 10\%$, CNO $\sim 2\%$. About $3 \cdot 10^{11}$ showers have been distributed in the zenith angle interval 0-60 degrees. The secondary particles have been propagated down to a cut-off energy of 1 MeV. The experimental conditions have been reproduced via a GEANT3-based code. The shower core positions have been randomly distributed sampling in energy-dependent area up to $10^3 \times 10^3 \text{ m}^2$, centered on the detector.

IV. DATA ANALYSIS

For the analysis of the shadowing effect a $10^\circ \times 10^\circ$ sky map in celestial coordinates (right ascension and declination) with $0.1^\circ \times 0.1^\circ$ bin size, centered on the Moon location, is filled with the detected events. The background is evaluated with both the *time swapping* [10] and the *equi-zenith angle* [11] methods.

With the time swapping method, N "fake" events are generated for each detected one, by replacing the measured arrival time with new ones. These events are randomly selected within a 3 hours wide buffer of recorded data. Swapping the time is swapping the right

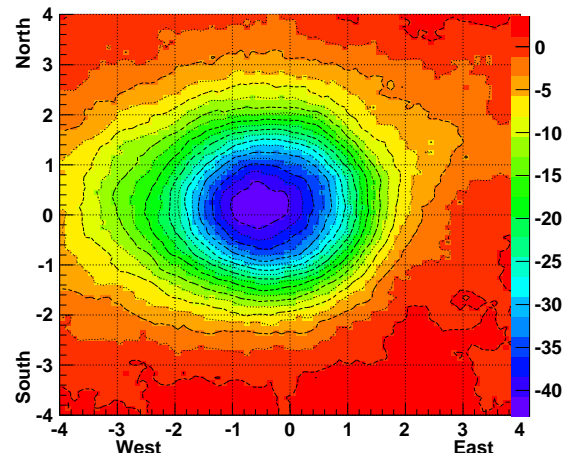


Fig. 1: Moon shadow significance map observed by the ARGO-YBJ detector in 2063 hours on-source for events with $N_{strip} \geq 30$ and zenith angle $\theta < 50^\circ$. The color scale gives the statistical significance.

ascension, keeping unchanged the declination. A new sky map (background map) is built by using 10 such fake events for each real one, so that the statistical error on the background can be kept small enough.

With the equi-zenith angle method 6 off-source bins are symmetrically aligned on both sides of the on-source field, at the same zenith angle. The off-source bins are each set at an azimuth distance $5^\circ/\sin\theta$ from the on-source bin, where θ is the zenith angle of the Moon position. Other off-source bins are located every $5^\circ/\sin\theta$ from the nearest off-source bins. The average of the event densities inside these bins was taken to be the background.

To maximize the signal to noise ratio, the bins are then grouped over a circular area of radius ψ , i.e. every bin is filled with the content of all the surrounding bins whose center is closer than ψ from its center. The value of ψ is related to the angular resolution of the detector, and corresponds to the radius of the observational window that maximizes the signal to noise ratio, which in turn depends on the number of fired pads of the event: when the PSF is a Gaussian with rms σ , $\psi = \sigma \cdot 1.58$ and contains $\sim 72\%$ of the events. Finally, the integrated background map is subtracted from the corresponding integrated event map, thus obtaining the "source map". For each bin of such a map, the deficit significance with respect to the background is calculated according to the Li and Ma formula [12]. Notice that in the integrated maps neighboring bins are correlated.

The analysis reported in this paper refers to events collected after the following event selection: (1) each event should fire more than 30 strips on the ARGO-130 central carpet to avoid any threshold effect; (2) the zenith angle of the shower arrival direction should be less than 50° ; (3) the reconstructed core position should be inside an area $250 \times 250 \text{ m}^2$ centered on the detector;

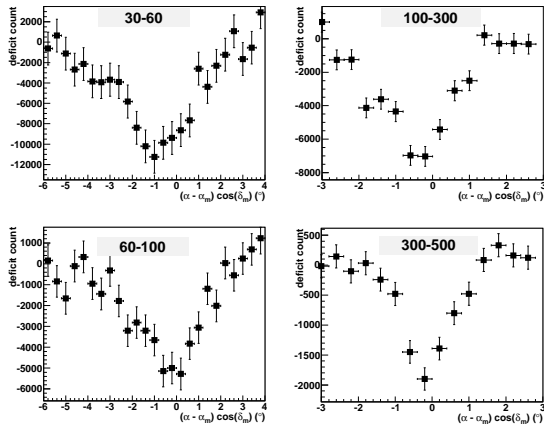


Fig. 2: Deficit counts measured around the Moon projected along the East-West axis for different multiplicity bins.

(4) the reduced χ^2 of the final temporal fit should be less than 100 ns^2 . According to our simulation studies, the median energy of the selected protons firing $30 \div 60$ strips is $E_{50} \approx 1.4 \text{ TeV}$ (mode energy $\sim 0.30 \text{ TeV}$).

In Fig.1 the Moon shadow observed with all data recorded since June 2006 (2063 hours on-source) for events with $N_{strip} \geq 30$ and zenith angle $\theta < 50^\circ$ is shown. The statistical significance of the observation is about 43 standard deviations.

V. RESULTS

The deficit counts observed around the Moon projected to the East-West axis are shown in Fig. 2 for 4 multiplicity bins. We use the events contained in an angular slice parallel to the East-West axis and centered to the observed Moon position. The widths of these bands are function of the N_{strip} -dependent angular resolution: $\pm 3.3^\circ$ in $30 \leq N_{strip} < 60$, $\pm 2.6^\circ$ in $60 \leq N_{strip} < 100$, $\pm 2.0^\circ$ in $100 \leq N_{strip} < 300$, $\pm 1.5^\circ$ in $300 \leq N_{strip} < 500$. As an expected effect of the geomagnetic effect, the profile of the shadow is broadened and the peak positions shifted westward as the multiplicity (i.e., the cosmic ray primary energy) decreases. We note that in the lowest multiplicity bin ($N_{strip} = 30 - 60$) the Moon is shifted by about 1° , as expected for a primary of rigidity $1.6 \text{ TeV}/Z$: this is the first time that an EAS-array is able to detect showers with such a low primary energy.

The best procedure to evaluate the pointing accuracy is to observe the position of the Moon shadow produced by high-energy cosmic rays which are negligibly affected by the geomagnetic field. For protons of 30 TeV we expect a deflection of about 0.05° . For heavier nuclei this deflection will increase but as the composition of cosmic rays in this energy range is dominated by the light component (nuclei heavier than CNO contribute to the rate less than 3% in the whole strip multiplicity range [13]) we expect only a small contribution from heavy ions to the blurring of the Moon shadow. As can be seen from the Fig. 3, the observed high energy ($N_{pad} \geq 1000$,

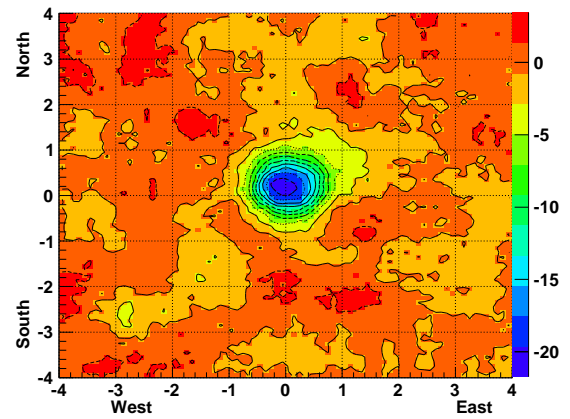


Fig. 3: Moon shadow significance map observed by the ARGO-YBJ detector in 2063 hours on-source for events with $N_{strip} \geq 1000$ and zenith angle $\theta < 50^\circ$. The color scale gives the statistical significance.

$E_p^{50} \sim 30 \text{ TeV}$) Moon shadow position is centered in the East-West direction but we observe a residual shift towards the North. Since the displacement along the North-South axis is not affected by the geomagnetic field at the Yangbajing latitude [9], we are able to investigate this pointing error without the Moon shadow simulation as a function of the multiplicity. The analysis has been performed both with the time-swapping and the equi-zenith angle methods: the results are in good agreement and suggest that there is a residual systematic shift towards North of $(0.20 \pm 0.05)^\circ$, independent of multiplicity. As a conservative estimate we assume our systematic errors to coincide with this displacement in both North-South and East-West projection. These upper limits for the systematic errors are however much smaller than our angular resolution, at least for the bulk of data, and can therefore be neglected in the point source searches.

In the Fig. 4 the displacement of the Moon shadow in the East-West direction is shown. Two different methods agree with each other quite well. A comparison between the measurement and the simulations allows to attribute this displacement to an absolute energy calibration of the detector.

The PSF of the detector, studied in the North-South projection, not affected by the geomagnetic field, is Gaussian for $N_{strip} \geq 100$, while for lower multiplicities it can be described with an additional Gaussian, which contributes for about 20%. For these events the angular resolution is calculated as the weighted sum of the σ^2 of each gaussian. In Fig. 5 the measured angular resolution is compared to expectations from a MC simulation as a function of the multiplicity. As can be seen, the values are in fair agreement: the angular resolution σ of the ARGO-YBJ experiment for cosmic ray-induced air showers is less than 0.6° for $N_{strip} \geq 300$. The effect of the finite angular width of the Moon on the angular

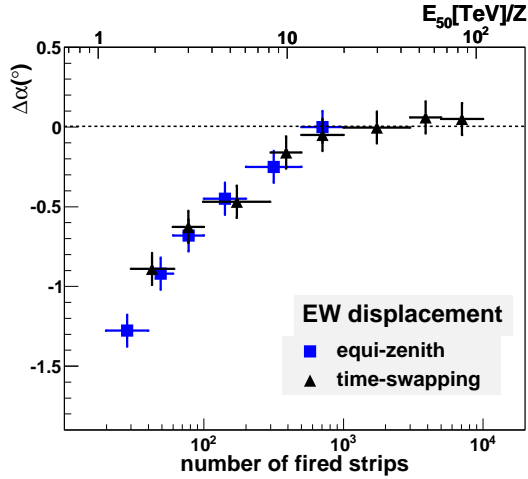


Fig. 4: Observed displacement of the Moon shadow in the East-West direction as a function of multiplicity. The upper scale refers to the median energy of rigidity (TeV/Z) in each multiplicity bin (shown by the horizontal errors). The experimental data calculated with two different methods (see text).

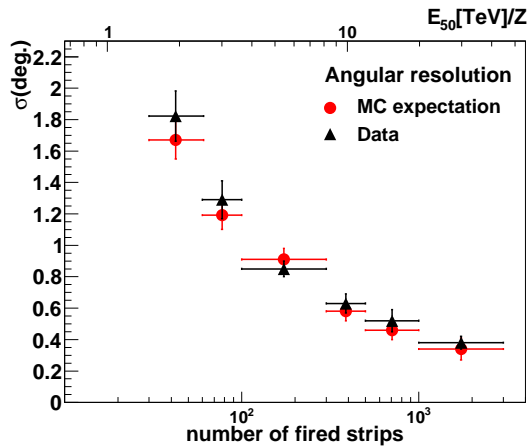


Fig. 5: Measured angular resolution of the ARGO-YBJ detector compared to expectations from MC simulation as a function of the multiplicity. The upper scale refers to the median energy of rigidity (TeV/Z) in each multiplicity bin (shown by the horizontal errors).

resolution (less than 5% if $\sigma > 0.4^\circ$ and only 1.7% if $\sigma > 0.7^\circ$) is discussed in [9]. From MC simulations we draw that the angular resolution for γ -induced showers at the threshold is at least 30% lower due to their better defined time profile [6]. A new reconstruction algorithm based on a weighted fit of the time profile is under study in order to improve the angular resolution.

A new reconstruction algorithm based on a weighted fit of the time profile is under study in order to improve the angular resolution.

VI. CONCLUSIONS

The galactic cosmic ray Moon shadowing effect has been observed by the ARGO-YBJ experiment in the

multi-TeV energy region with high statistical significance. The analysis has been performed both with the time-swapping method and the equi-zenith angle method in order to investigate possible biases in the background calculation. The measured angular resolution is in good agreement with MC simulations, making us confident in the reconstruction algorithms, we can further find an absolute energy calibration of the detector.

REFERENCES

- [1] D.E. Alexandreas et al., *Phys. Rev.* **D43** 1735, 1991.
- [2] G.W. Clark, *Phys. Rev.* **108** 450, 1957.
- [3] M. Amenomori et al., *ApJ* **541** 1051, 2000.
- [4] F.R. Zhu et al., these proceedings
- [5] G. Aielli et al., *NIM* **A562** 92, 2006.
- [6] G. Di Sciascio et al., Proc. of *30th ICRC* 2009, (preprint: arXiv:0710.1945).
- [7] D. Heck et al., Report **FZKA 6019** 1998.
- [8] B. Wiebel-Sooth et al., *A&A* **330** 389, 1998.
- [9] G. Di Sciascio and R. Iuppa, these proceedings
- [10] D.E. Alexandreas et al., *NIM* **A311** 350, 1992.
- [11] M. Amenomori et al., *Phys. Rev.* **D47** 2675, 1993.
- [12] T. Li and Y. Ma, *ApJ*, **272** 317, 1993.
- [13] S. Catalanotti et al., these proceedings.